# High temperature diffraction study of in-situ crystallization of nanostructured $TiO_2$ photocatalysts

**J.M. Low[1*], B. Curtain[1], M. Philipps[1], Z.Q. Liu[2] and M. Ionescu[3]**

1) Centre for Materials Research, Curtin University, GPO Box U1987, Perth, WA 6845, Australia
2) School of Chemical Engineering, Sichuan University, China
3) Australian Nuclear Science and Technology Organisation, Sydney NSW 2234, Australia

Email: j.low@curtin.edu.au

Available Online at: www.austceram.com/ACS-Journal

**Abstract**
The in-situ crystallization of anatase and rutile on chemically-treated Ti-foils in the temperature range 20-900ºC has been investigated using synchrotron radiation diffraction and x-ray diffraction. The processing methodology has a profound influence on the morphology, crystallite size and growth rate of nanostructured $TiO_2$. The anatase formed was metastable and transformed to rutile at ~800ºC. Increasing the temperature from 400 to 900ºC caused the sharpening of anatase (101) peaks and resulted in a concomitant coarsening in crystallite size. The surface of annealed samples exhibited $TiO_2$ nanorods, nanowires or nanotubes depending on the processing method. Ion-beam analysis has indicated the existence of composition gradation within the annealed $TiO_2$ samples at the near-surface.

**Keywords**: Anatase, rutile, photocatalyst, nanotubes, diffraction analysis, ion-beam analysis

## INTRODUCTION

$TiO_2$ is currently used in a number of fascinating applications, including as photocatalysts. In particular, there is great interest in using $TiO_2$ nanotubes because of the added surface areas available. Due to its high photoactivity, photodurability, chemical and biological inertness, mechanical robustness and low cost, nanostructured semiconducting $TiO_2$ has attracted much more attention for its potential applications in diverse fields such as photocatalysis of pollutant [1], photo-splitting of water [2-4] and transparent conducting electrodes for dye-sensitized solar cells [5]. Since photocatalytic reactions mainly take place on the surface of the catalyst, a high surface-to-volume ratio is of great significance for increasing the decomposition rate. Very high photocatalytic activity has already been demonstrated for nanostructured $TiO_2$ with various morphologies such as nano-powders [1-5], nano-rods [6], nano-wires [7], nano-fibers [8-9], nano-belts [10], nano-tubes [11], thin films [12], and porous nanostructures [13-15]. Although a lot of progress has been achieved in these forms of $TiO_2$, the poor recuperability and reutilization limitation for nano-powders and processing difficulty for nano-fibres or nano-tubes are still challenges for their commercial applications.

Hitherto, various processes of materials synthesis have been developed for nanostructured $TiO_2$ and these include the sol-gel method [16], micelles and inverse micelles method [17], hydrothermal method [18], and the solvothermal method [19]. Using indirect oxidation methods, nanorod arrays have been prepared on the surface of Ti substrates by oxidizing titanium with $(CH_3)_2CO$ [20], $H_2O_2$ solution [21], and KOH [22]. However, few literature sources have reported the growth of aligned $TiO_2$ nanostructures on the substrate by electrochemical anodization of Ti metal and subsequent annealing in air. In this paper, we have described four methodologies to synthesize nanostructured $TiO_2$ with various morphologies. The effect of processing methodology on the morphologies of $TiO_2$ and their structure-property relations are discussed.

## EXPERIMENTAL METHODS

### Sample Preparation

Four methods were used to synthesize $TiO_2$ of various nanostructured morphologies from chemical treatments of Ti foils (99.7% purity). These methods were (a) Ti foil was initially cleaned using 2M HCl

and deionised water. The cleaned foil was then oxidized in 30% $H_2O_2$, followed by annealing in an oven at 80°C for 72 h; (b) The cleaned foil was etched with 2M HF; (c) The cleaned foil was etched with 2M HCl. After etching, samples were annealed for 6 hours at 450°C, 500°C, 550°C, 600°C and 650°C; and (d) the cleaned foil was anodized in an electrolyte of $H_3PO_4/NH_4F$ [23]. The process of potentiostatic anodization was performed in a standard two-electrode electrochemical cell, with Ti as the working electrode and platinum as the counter electrode. The anodization process was performed under an applied voltage of 20 V for 3.0 h. Both as-etched and as-anodized Ti-foils were used for the in-situ study of phase transformation at elevated temperature using either synchrotron radiation diffraction or laboratory x-ray diffraction.

The morphologies of the as-prepared and heat-treated Ti foils were characterized using a field emission scanning electron microscope (FESEM SUPRA 35VP ZEISS) operating at working distances of 5 mm with an accelerating voltage of 5 kV.

**In Situ High-Temperature X-Ray Diffraction**

In this study, the in-situ oxidation behaviour of as-etched and anodized Ti-foils was characterised using high-temperature laboratory x–ray (XRD) or synchrotron radiation diffraction (SRD) up to 900 °C in air. These measurements were conducted at ANSTO and the Australian Synchrotron respectively. The high-temperature diffraction data were collected using an Anton Parr HTK20 furnace and the Mythen II microstrip detector. The XRD and SRD data were collected at a wavelength of 0.15407 nm and 0.11267 nm respectively.

The diffraction patterns were acquired in steps of 100 °C from 200 °C to 400 °C and thereafter every 50 °C from 200 °C to 900 °C. The collected diffraction data were analysed to compute the relative phase abundances of oxides formed at each temperature. The mean crystallite size ($L$) of $TiO_2$ was calculated from (101) reflections of anatase using the Scherrer equation [24]:

$$L = \frac{K\lambda}{\beta \cos\theta} \qquad (1)$$

where $K$ is the shape factor, $\lambda$ is the x-ray wavelength, $\beta$ is the line broadening at half the maximum intensity (FWHM) in radians, and $\theta$ is the Bragg angle.

**Ion-Beam Analysis (IBA)**

Ion beam analysis is a procedure where a focussed beam of ions (typically He+ ions) is shot at a sample surface. In doing so, particles from the bombarded surface interact with the incoming ions. Rutherford backscattering spectrometry (RBS) uses the ion beam interaction to provide information on the concentration versus depth for elements. Depending on the sample atomic structure, the $He^+$ ions are backscattered from the surface due to repulsion from the nuclei of larger atoms (e.g. Ti). By measuring the energy of the repelled ions, information on the composition of the elements and their depth within the sample can be collected. Using this procedure the depth of the surface oxide layer can be studied by comparing the relative concentrations of Titanium and Oxygen versus depth. This work conducted at the Australian Nuclear Science & Technology Organisation (ANSTO) using 1.8MeV $He^{1+}$ ions on the 2MV tandem accelerator.

## RESULTS AND DISCUSSION

**In-Situ Formation of $TiO_2$ at Elevated Temperature**

Fig. 1 shows the formation of anatase on Ti-foil etched in $H_2O_2$ followed by annealing at 80°C for 72 h. The ability of $H_2O_2$ to readily oxidize Ti is evident. However, when the Ti-foil was etched by either HF or HCl, no anatase formed at all and rutile only crystallized at 700°C (see Fig. 2).

Fig. 3 shows the initial formation of metastable anatase in as-anodized Ti-foil at room temperature which eventually transformed to rutile after thermal annealing in air at 900°C. The as-anodized $TiO_2$ nanotube arrays were crystalline in nature rather than amorphous and the metastable anatase formed during anodization did not transform to rutile until 800°C [see Fig. 4.] The corresponding variations of phase abundances in titanium, anatase and ruile as a function of temperature are shown in Fig. 5. It is interesting to note that the formation of rutile resulted in the concomitant reduction in the phase abundance of anatase and titanium.

However, it is well-known that anatase undergoes a phase transformation to rutile at ~500-550 °C [25-27]. However, the much higher temperature of anatase to rutile transition observed in this study can be attributed to the thickness of Ti-foil being too thick for efficient heat-transfer, resulting in the undesirable thermal gradient on the sample.

Although anatase was observed up to 900°C, there was a distinct narrowing and sharpening in the (101) peak, resulting in a corresponding decrease in the values of full-width half-maximum (FWHM) as the temperature increased. From the Scherrer equation [24], a decrease in the value of FWHM implies an

increase in the mean crystallite size for anatase. Fig. 6 shows the influence of annealing temperature on crystallite size for anatase formed by different processing methodologies. In the case of anodized $TiO_2$, the crystallite size of anatase was about 32 nm at 400 °C and increased very gradually with temperature to 40 nm at 900 °C. Faster growth rates were observed for anatase synthesized from treatment with HF and $H_2O_2$ although their crystallite sizes were much smaller, especially for the latter. Another feature worth-noting in Figs. 2 & 3 is the lack of line-shifts in the peaks as the temperature increases due to thermal expansion. This may imply that the nanostructured $TiO_2$ formed have a very low coefficient of thermal expansion due to their high porous microstructure.

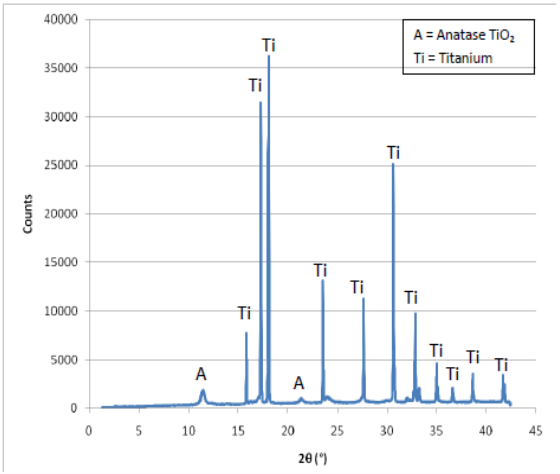


Fig. 1: SRD pattern of Ti-foil etched with $H_2O_2$ and annealed at 80°C for 72 h.

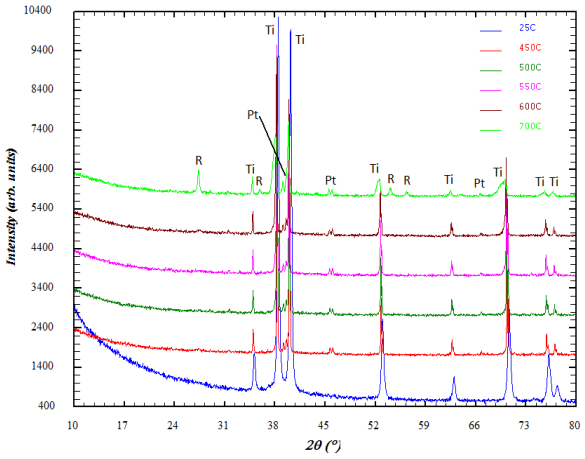


Fig. 2: In-situ high-temperature XRD patterns of Ti-foil etched with 2M HF.

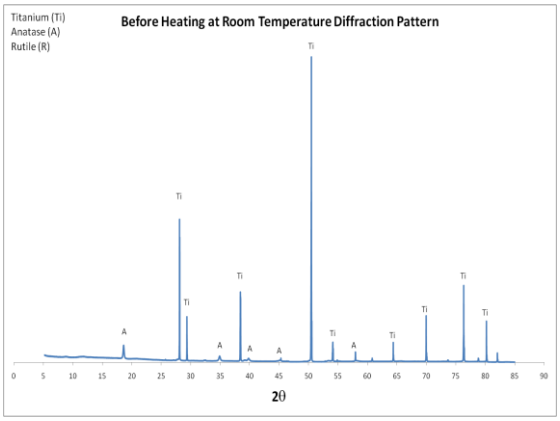


(a)

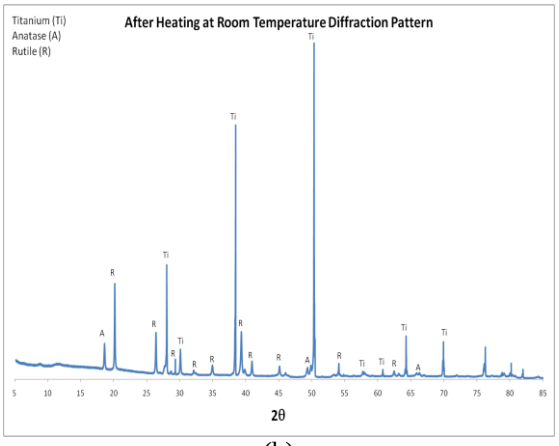


(b)

Fig. 3: Synchrotron radiation diffraction plots of as-anodized $TiO_2$ (a) before annealing at 20ºC and (b) after annealing at 900ºC.

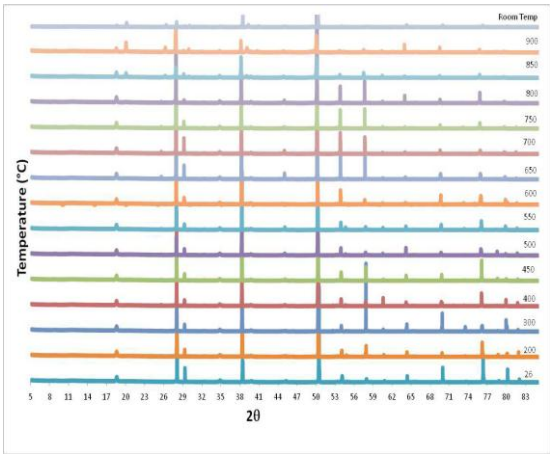


Fig. 4: Synchrotron radiation diffraction plots showing phase transitions during in-situ annealing of as-anodized $TiO_2$ in the temperature range 20-900 ºC.

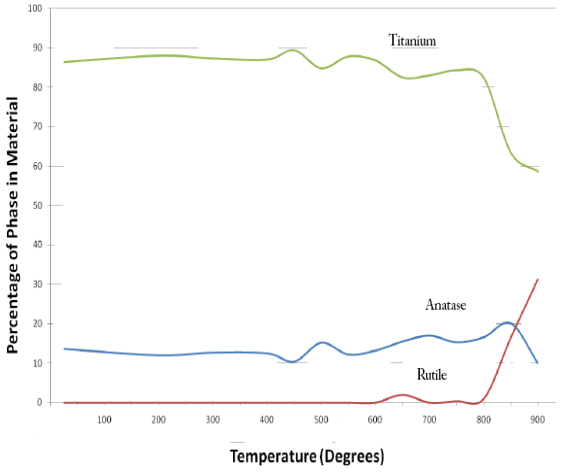


Fig. 5: Phase abundances of Ti, anatase and rutile in anodized $TiO_2$ as a function of temperature.

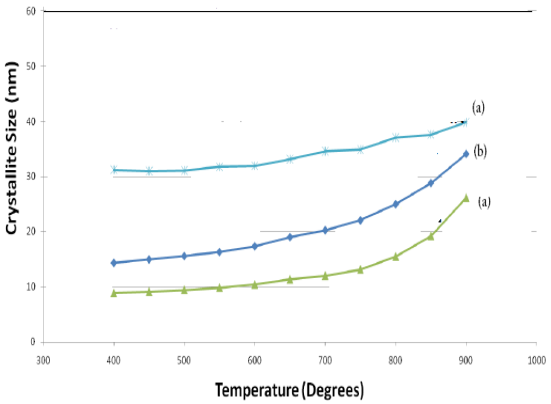


Fig. 6: Variations of crystallite size as a function of temperature for anatase synthesized from (a) anodization in $H_3PO_4/NH_4F$, (b) HF etching, and (c) $H_2O_2$ oxidation.

**Microstructures of Nanostructured $TiO_2$**

Figure 7 shows the profound influence of processing methodologies on the morphologies of the synthesized $TiO_2$. Fine nanorods can be observed for the sample prepared by $H_2O_2$ oxidation whereas wire-like nanostructures are formed the sample etched by HF (Fig. 7b). In contrast, vertically oriented and highly ordered arrays of anatase nanotubes with diameter of ~80 nm and wall thickness of 20 nm formed in the sample anodized in $H_3PO_4/NH_4F$ (Fig. 7c) for 3 h. These results are in good agreement with similar studies reported for anodized $TiO_2$ [28-32].

Three simultaneously occurring processes can be ascribed to the formation of the nanotube arrays in fluoride containing electrolyte [31]. The first involves the field-assisted oxidation of Ti metal to form $TiO_2$, which is followed by field-assisted dissolution of Ti metal ions in the electrolyte, and finally the chemical dissolution of Ti and $TiO_2$ in the presence of hydrogen and fluoride ions. Plausible pathways of chemical reaction occurring during anodization are as follows:

$$Ti_{(s)} \rightarrow Ti^{4+}_{(aq)} + 4e^-$$
$$Ti^{4+}_{(aq)} + 4F^-_{(aq)} \rightarrow TiF_{4\,(aq)}$$
$$TiF_{4\,(aq)} + 2H_2O_{(aq)} \rightarrow TiO_{2\,(s)} + 4HF_{(aq)}$$

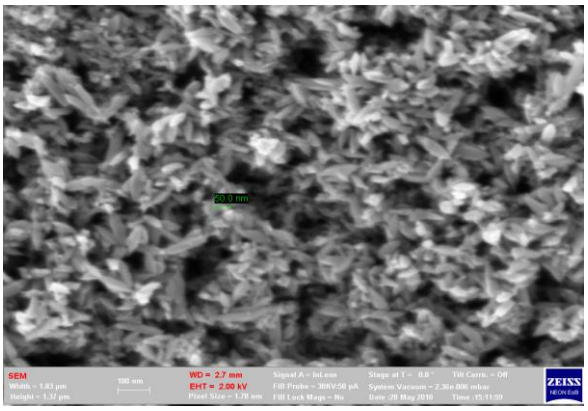

(a) Nanorods

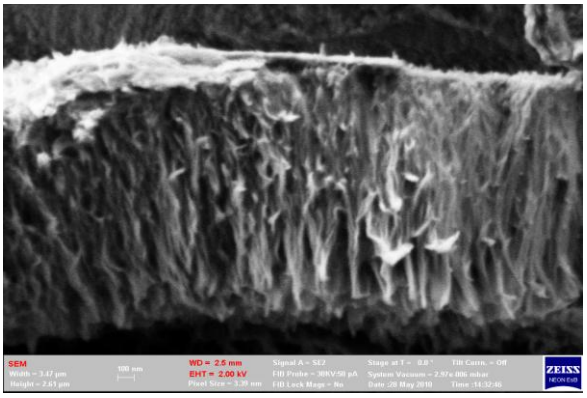

(b) Nanowires

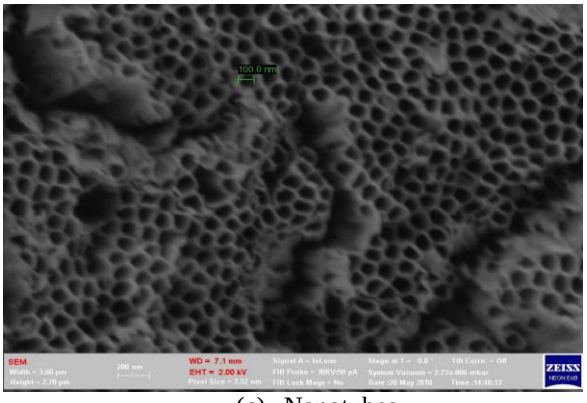

(c) Nanotubes

Fig. 7: Scanning electron micrographs showing the microstructure of nanostructured $TiO_2$ synthesized from (a) $H_2O_2$ oxidation, (b) HF etching and (c) anodization in $H_3PO_4/NH_4F$.

**Composition Depth-Profiles**

The typical composition depth profiles of oxygen and titanium at the near-surface of samples prepared by different methodologies are shown in Fig. 8. As would be expected, a large graded concentration of oxygen existed on all the samples at the near-surface as a result of chemical solution treatment and subsequent oxidation by thermal annealing.

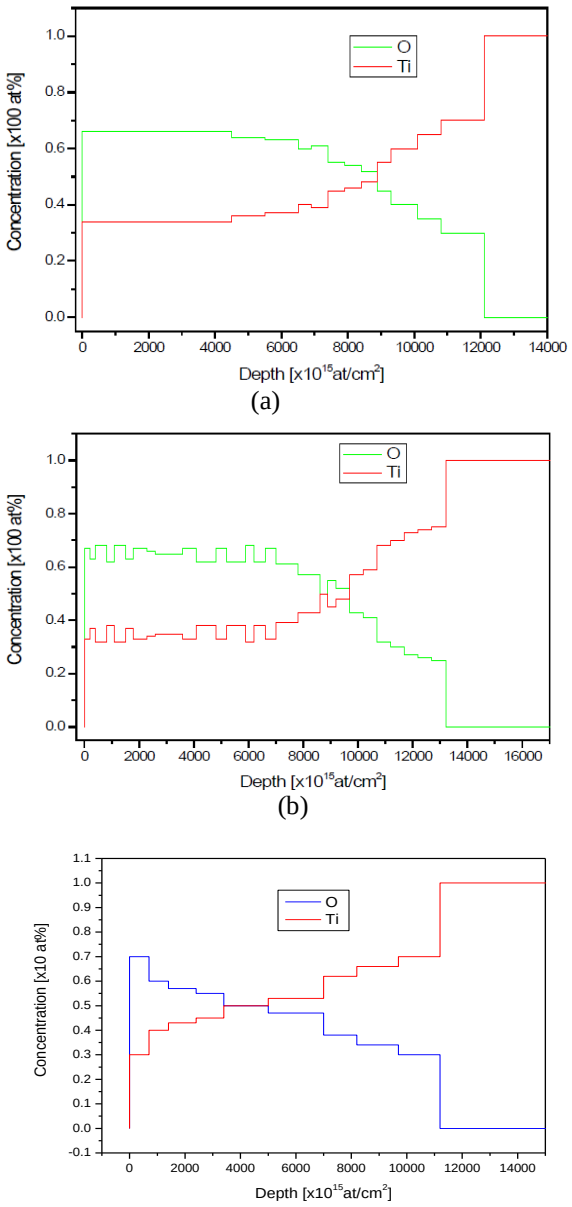


Fig. 8: Depth-profiling results obtained from ion-beam analyses of samples synthesized by (a) HF, (b) HCl, and (c) anodization in $H_3PO_4/NH_4F$

It is quite reasonable to assume that the point at which the titanium content exceeded the oxygen content corresponds to the depth of the $TiO_2$ layer formed on the sample. Based on this assumption, the depths of the graded $TiO_2$ layers formed from HF and HCl etching are very similar but a thinner oxide layer formed in the anodized sample. This difference in thickness of oxide layers may be attributed to higher annealing temperature (i.e. 600ºC versus 400ºC) used. Since the processes of oxidation and growth of oxides are diffusion-controlled, a higher annealing temperature will result in much faster growth of $TiO_2$ and thus the thickness of the graded oxide layer.

The effect of annealing temperature on the growth and thickness of oxide layers in samples prepared by HF and HCl etching is shown in Figure 9. Initially the oxide layers in both samples appeared to show very similar growth rates or thickness at 450-500ºC but as the annealing temperature increased beyond 500ºC the oxide layer from HF-etching appeared to grow faster than the HCl-etched sample.

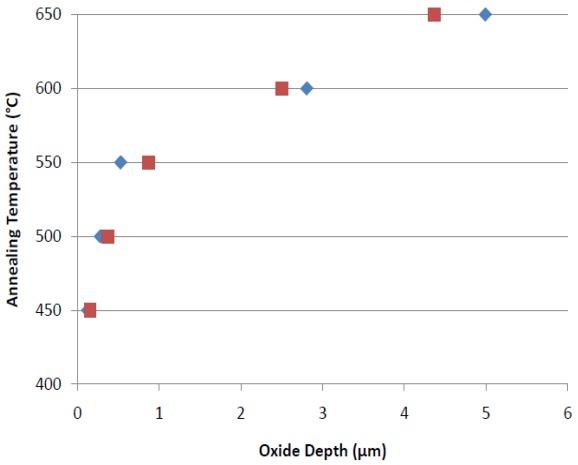


Fig. 9: Effect of annealing temperature on the depth of oxide layer formed in samples etched with HF(♦) and HCl (■).

## CONCLUSIONS

Nanostructured $TiO_2$ with various morphologies have been modified from Ti foils processed by four different methodologies. The surface of samples exhibited $TiO_2$ nanorods, nanowires or nanotubes depending on the processing method used. The processing methodology has a profound influence on the morphology, crystallite size and growth rate of nanostructured $TiO_2$. The in-situ crystallization of anatase and rutile in the temperature range 20-900ºC was investigated using synchrotron radiation diffraction and x-ray diffraction. Metastable anatase formed in samples prepared by $H_2O_2$ oxidation and anodozation but not in the HF or HCl-etched samples. Transformation from anatase to rutile occurred at ~800ºC. Increasing the temperature from 400 to

900ºC caused the sharpening of anatase (101) peaks and resulted in a concomitant coarsening in crystallite size. Ion-beam analysis has indicated the existence of composition gradation within the annealed $TiO_2$ samples at the near-surface.

**ACKNOWLEDGMENTS**

This work was supported by funding from the Australian Synchrotron (AS102/PD/1654 & AS102/PD/2494), the Australian Institute of Nuclear Science and Engineering (AINGRA10127). We thank Ms E. Miller of Curtin Centre for technical assistance with the SEM work.

**REFERENCES**

1. M.R. Hoffmann, S.T. Martin, W. Choi and D.W. Bahnemann, "Environmental Applications of Semiconductor Photocatalysis", Chem. Rev., Vol. [95], (1995) 69-96.
2. A. Fujishma, K. Honda, "Electrochemical Photolysis of Water at a Semiconductor Electrode", Nature, Vol. [238], (1972) 37.
3. Y.B.Liu, B.X. Zhou, J. Bai, J.H. Li and X.L. Zhang, "Efficient Photochemical Water Splitting and Organic Pollutant Degradation by Highly Ordered $TiO_2$ Nanopore Arrays", Appl. Catal. B, Vol. [89], (2009) 142-148.
4. E. Indrea, S. Dreve, T.D. Silipas, G. Mihailescu, V. Danciu, V. Cosoveanu, A. Nicoara, L.E. Muresan, E.J. Popovici, V. Popescu, H.I. Nascu and R. Tetean, "Nanocrystalline Semiconductor Materials for Solar Water-Splitting", J. Alloys Compd., Vol. [483], (2009) 445-449.
5. B. O'Regan, M. Grätzel, A Low-Cost, High-Efficiency Solar Cell Based on Dye-Sensitized Colloidal $TiO_2$ Films, Nature, Vol. [353], (1991) 737-740.
6. H. Cheng, J. Ma, Z. Zhao and L. Qi, "Hydrothermal Preparation of Uniform Nanosize Rutile and Anatase Particles", Chem. Mater., Vol. **7**, (1995) 657-671.
7. Z. Miao, D. Xu, J. Ouyang, G. Guo, X. Zhao, and Y. Tang, "Electrochemically Induced Sol−Gel Preparation of Single-Crystalline $TiO_2$ Nanowires", Nano Lett., Vol. [2], (2002) 717-720.
8. Y.G. Guo, J. Hu, H. Liang, L. Wan and C. Bai, "$TiO_2$-Based Composite Nanotube Arrays Prepared via Layer-by-Layer Assembly", Adv. Funct. Mater., Vol. [15], (2005) 196-202.
9. Y. Zhang, Y. Gao, X.H. Xia, Q.R. Deng, M.L. Guo, L. Wan and G. Shao, "Structural Engineering of Thin Films of Vertically Aligned $TiO_2$ Nanorods", Mater. Lett., Vol. [14], (2010) 1614-1617.
10. Y.M. Wang, G. Du, H. Liu, D. Liu, S. Qin, N. Wang, C. Hu, X. Tao, J. Jiao, J. Wang and Z.L. Wang, "Nanostructured Sheets of $TiO_2$ Nano-Belts for Gas Sensing and Antibacterial Applications", Adv. Func. Mater., Vol. [18], (2008) 1131-1137.
11. Z.R. Tian, J.A. Voigt, J. Liu, B. Mckenzie, and H. Xu, "Large Oriented Arrays and Continuous Films of $TiO_2$ Based Nanotubes", J. Am. Chem. Soc., Vol. [125], (2003) 12384-12385.
12. R. Asahi, T. Morikawa, T. Ohwaki, K. Aoki and Y. Taga, "Visible-Light Photocatalysis in Nitrogen-Doped Titanium Oxides", Science, Vol. [293], (2001) 269-271.
13. P.D. Yang, D. Y. Zhao, D. Margolese, B.F. Chmelka and G.D. Stucky, "Generalized Syntheses of Large-Pore Mesoporous Metal Oxides with Semicrystalline Frameworks", Nature, Vol. [396], (1998) 152-155.
14. U.M. Patil, K.V. Gurav, O.S. Joo and C.D. Lokhande, "Synthesis of Photosensitive Nanograined $TiO_2$ Thin Films by SILAR Method", J. Alloys Compd., Vol. [478], (2009) 711-715.
15. Y. Shen, J. Tao, F. Gu, L. Huang, J. Bao, J. Zhang and N. Dai, "Preparation and Photoelectric Properties of Ordered Mesoporous Titania Thin Films", J. Alloys Compd., Vol. [474], (2009) 326-329.
16. J. Tang, F. Redl, Y. Zhu, T. Siegrist, L.E. Brus, and M.L. Steigerwald, "An Organometallic Synthesis of $TiO_2$ Nanoparticles", Nano Lett., Vol. [5], (2005) 543-548.
17. G.L. Li, and G. H. Wang, "Synthesis of Nanometer-Sized $TiO_2$ Particles by a Microemulsion Method", Nanostruct. Mater., Vol. [11], (1999) 663-668.
18. Q. Huang, L. Gao, "A Simple Route for the Synthesis of Rutile $TiO_2$ Nanorods", Chem. Lett., Vol. [32], (2003) 638-640.
19. X. Wang, J. Zhuang, Q. Peng and Y. Li, "A General Strategy for Nanocrystal Synthesis", Nature, Vol. [437], (2005) 121-124.
20. X. Peng, A. Chen, "Aligned $TiO_2$ Nanorod Arrays Synthesized by Oxidizing Titanium with Acetone", *J.* Mater. Chem., Vol. [14], (2004) 2542-2548.
21. J.M. Wu, "Low-Temperature Preparation of Titania Nanorods through Direct Oxidation of Titanium with Hydrogen Peroxide", J. Cryst. Growth, Vol. [269], (2004) 347-355.

22. M. Asadi, M. Attarchi, M. Vahidifar, A. Jafari, "Film Formation via Plasma Electrolyte Oxidation of Ti and Ti-5Mo-4V-3Al Alloy in High Alkaline Solutions", Defect and Diffusion Forum, Vol. [297-301], (2010) 1167-1170.
23. Z. Liu, X. Yan and D. Li, "Effects of Impurities Containing Phosphorous on the Surface Properties and Catalytic Activity of $TiO_2$ Nanotube Arrays", Appl. Surf. Sci., Vol. [257], (2010) 1295-1299.
24. B.D. Cullity and S.R. Stock, *Elements of X-Ray Diffraction*, 3rd Ed., Prentice-Hall Inc., pp. 167-171 (2001)
25. S. Sreekantan, R. Hazaan, Z. Lockman, "Photoactivity of Anatase-Rutile $TiO_2$ Nanotubes Formed by Anodization Method", Thin Solid Films, Vol. [518], (2009) 16-21.
26. I.M. Low, E. Wren, K.E. Prince and A. Anatacio, "Characterisation of Phase Relations and Properties in Air-Oxidised $Ti_3SiC_2$", Mater. Sci. Eng. A., Vol. [466], (2007) 140-147.
27. W.K. Pang, I.M. Low, B.H. O'Connor, K.E. Prince and A. Anatacio, "Oxidation Characteristics of $Ti_3AlC_2$ over Temperature Range 500-900$^oC$", Mater. Chem. Phys., Vol. [117], (2009) 384-389.
28. X. Meng, T.Y. Lee, H. Chen, D.W. Shin, K.W. Kwon, S.J. Kwon, J.B. Yoo, "Fabrication of Free Standing Anodic Titanium Oxide Membranes with Clean Surface Using Recycling Process", J. Nanosci. & Nanotech., Vol. [10], (2010) 4259–4265.
29. V.M. Prida, M. Hernandez-Velez, K R Pirota, A. Menendez and M. Vazquez, "Synthesis and Magnetic Properties of Ni Nano-Cylinders in Self-Aligned and Randomly Disordered Grown Titania Nanotubes", Nanotechnology, Vol. [16], (2005) 2696–2702.
30. O.K. Varghese, D. Gong, M. Paulose, C.A. Grimes, E.C. Dickeya, "Crystallization and High-Temperature Structural Stability of $TiO_2$ Nanotube Arrays", J. Mater. Res., Vol. [18], (2003) 156-165.
31. Y. Zhang, W. Fu, H. Yang, Q. Qi, Y. Zeng, T. Zhang, R. Ge, G. Zou, "Synthesis and Characterization of $TiO_2$ Nanotubes for Humidity Sensing", Appl. Surf. Sci., Vol. [254], (2008) 5545–5547.
32. K. Mor, O. K. Varghese, M. Paulose, K. Shankar, C. A. Grimes, "A Review on Highly Ordered, Vertically Oriented $TiO_2$ Nanotube Arrays: Fabrication, Material Properties, and Solar Energy Applications", Solar Energy Mat. Solar Cells, Vol. [90], (2006) 2011-2075.